

Article

Fire Resistance and Mechanical Properties of Intumescent Coating Using Novel BioAsh for Steel

Jing Han Beh ^{1,*}, Ming Chian Yew ^{2,*} , Lip Huat Saw ² and Ming Kun Yew ³

¹ Department of Architecture and Sustainable Design, Lee Kong Chian Faculty of Engineering and Science, Universiti Tunku Abdul Rahman, Cheras, Kajang 43000, Malaysia

² Department of Mechanical and Material Engineering, Lee Kong Chian Faculty of Engineering and Science, Universiti Tunku Abdul Rahman, Cheras, Kajang 43000, Malaysia; sawlh@utar.edu.my

³ Department of Civil Engineering, Lee Kong Chian Faculty of Engineering and Science, Universiti Tunku Abdul Rahman, Cheras, Kajang 43000, Malaysia; yewmk@utar.edu.my

* Correspondence: behjh@utar.edu.my (J.H.B.); yewmc@utar.edu.my (M.C.Y.);
Tel.: +60-3-0986-0288 (J.H.B. & M.C.Y.)

Received: 6 October 2020; Accepted: 3 November 2020; Published: 20 November 2020



Abstract: Recent developments of intumescent fire-protective coatings used in steel buildings are important to ensure the structural integrity and safe evacuation of occupants during fire accidents. Flame-retardant intumescent coating applied to structural steel could delay the spread of fire and heat propagation across spaces and structures in minimizing fire risks. This research focuses on formulating a green intumescent coating utilized the BioAsh, a by-product derived from natural rubberwood (hardwood) biomass combustion as the natural substitute of mineral fillers in the intumescent coating. Fire resistance, chemical, physical and mechanical properties of all samples were examined via Bunsen burner, thermogravimetric analysis (TGA), carbolite furnace, scanning electron microscopy (SEM), energy dispersive X-ray spectroscopy (EDX), Fourier transform infrared (FTIR), freeze–thaw cycle, static immersion and Instron pull-off adhesion test. Sample BioAsh intumescent coating (BAIC) 4-7 incorporated with 3.5 wt.% BioAsh exhibited the best performances in terms of fire resistance (112.5 °C for an hour under the Bunsen burner test), thermal stability (residual weight of 29.48 wt.% at 1000 °C in TGA test), adhesion strength (1.73 MPa under Instron pull-off adhesion test), water resistance (water absorption rate of 8.72%) and freeze–thaw durability (no crack, blister and color change) as compared to other samples. These results reveal that an appropriate amount of renewable BioAsh incorporated as natural mineral fillers into the intumescent coating could lead to better fire resistance and mechanical properties for the steel structures.

Keywords: intumescent coating; flame-retardant; fire resistance; rubberwood ash; mineral fillers; mechanical properties

1. Introduction

The fire resistance of materials is one of the key fire safety measures in building design and the construction industry—it must comply with BS 476. Fire safety rules and regulations in the building are important to reduce deaths and serious injuries [1–4]. Intumescent coating (IC) has been used as a passive fire protection design measure in the building industry especially to protect steel structures from fire damage [5,6]. Flame-retardant IC can ensure structural integrity by providing a protective barrier to building materials from reaching a critical temperature when exposed to fire. IC can delay the propagation of fire and maintain enough time for the safe evacuation of occupants during a fire incident [7]. The fire-protective mechanism of IC is working via the formation of uniform multicellular char layer, which proves the ability to delay the speed of heat transfer to the building structure. In this

research, vinyl acetate-ethylene copolymer (VAC) emulsion was chosen as the binder for BioAsh IC samples due to its more eco-friendly, less flammable and has lower volatile organic contents as compared to the solvent-based binder. It is also less hazardous and harmful to the environment and is able to offer good adhesion strength and humidity resistance [8]. However, direct and continuous exposure of VAC binder to moisture will affect its chemical bonding and weakens the adhesion strength [9]. The binder used in the IC is crucial because it assists in the expansion of char and ensures the formation of a uniform char foam structure, which acts as an insulating layer to protect the substrate [10,11]. Hydrophilic fire-retardant additives such as ammonium polyphosphate (APP) and pentaerythritol (PER) in the IC are sensitive to corrosive components like water, acid, and alkali. These additives could easily migrate to the coating's surface when exposed to a corrosive environment. These phenomena will significantly suppress the performance of IC. VAC copolymer binder used in the IC can limit the migration of flame-retardant additives from accessing the corrosive substances [12–14].

IC consists of three main halogen-free flame-retardant additives: ammonium polyphosphate (APP), an acid source, melamine (MEL), a blowing agent, and pentaerythritol (PER), a charring agent [15]. (1) An acid source such as inorganic acid, acid salt or other acids that elevate the dehydration of carbonizing agent; (2) a carbonizing agent which is a carbohydrate that will be dehydrated by the acid source to become a char; (3) a blowing agent that will be decomposed to release gas resulting in the increase in polymer's volume and the formation of a swollen multi-cellular layer to protect the steel underneath from fire [16]. This will tremendously reduce the structural degradation of buildings during fire events. Industrial mineral fillers such as titanium dioxide, magnesium hydroxide and aluminium hydroxide are vital flame-retardant ingredients added into IC to enhance the fire-resistance performance. There is no adverse effect reported on toxic smoke leading to death or injury in fire using flame-retardant mineral fillers. The decomposition temperature of flame-retardant fillers to polymer is important to optimize the use of mineral fillers. Factors such as the coherency of the residual layer and its tendency to recondense thermal emission are also needed to be considered [17]. In this research, BioAsh was incorporated as green mineral filler to partially replace the use of industrial flame-retardant fillers in the IC.

Incorporation of novel BioAsh into IC samples was emphasized in this research. BioAsh was derived from rubberwood biomass combustion obtained from a fuel-burning factory located in Sitiawan, Perak, Malaysia. BioAsh was the residual of the burning activity of rubberwood biomass. Rubberwood biomass was left over from rubber tree logging activities. *Hevea brasiliensis* (rubberwood) is a type of hardwood tree species commercially planted in Malaysia for latex cultivation. Malaysia is the fifth largest rubber producer and exporter in the world [18], with rubber plantations occupied at about 1.07 million hectares land areas in the country [19]. The logging of rubberwood when they reach the end of latex secretion cycle left a large amount of biomass. These rubberwood biomasses are readily available to use as bioenergy or biofuel for factories. Combustions of biomass produce a relatively large amount of BioAsh. BioAsh is derived from the biomass combustion of natural rubber wood in this research. Most of the BioAsh generated by biomass combustion will be considered as a type of industrial waste and will be disposed to landfill at a certain cost [20]. Environment hazards would be minimized by utilizing renewable BioAsh in the green IC as initiated by this research due to its eco-compatible filler.

In general, wood-based ash was identified with several minerals, such as carbon, calcium, potassium, magnesium, phosphorus, and sodium [21]. Wood ash is also identified with compounds such as silicon dioxide, aluminium hydroxide, ferric oxide, calcium oxide, magnesium oxide, titanium dioxide, potassium oxide and sulfur trioxide. Most of the decomposed elements possess high thermal degradation after the pyrolysis. Hemicellulose, cellulose and lignin were reported in plant-based materials and thermal degradation varied [22]. Wood ash that is rich in pozzolan is also used as partial cement replacement for building materials in the construction industry. A pozzolan is a material rich in silica and alumina that will react with calcium hydroxide Ca(OH)_2 , forming a cementitious-like compound with the presence of moisture [23]. The physical and chemical properties

of wood ash are depending on factors such as wood species, types of wood, combustion method, combustion temperature and soil condition. Combustion of hardwood tree species will obtain more ash than softwood species and the yield of wood ash will decrease when burning temperature raising. Many types of research have been done to examine different mix proportion of binder, flame-retardant additives, and fillers to enhance the fire resistance performance of IC [24–53].

Conventional IC reported an average equilibrium temperature of 160–190 °C (epoxy-based) and 220–290 °C (water-based) when the steel substrate was exposed to 1000 °C heat in the fire test [37,48,52,53]. Advanced studies have been conducted to explore the potential of various aviculture waste (eggshell), agriculture waste (rice husk ash), aquaculture waste (clam shell) and crop-based biomass (ginger powder and coffee husk) to produce eco-compatible IC formulations with enhanced fire-resistant performance [48,51–53]. These studies of using natural-based fillers in the IC reported various improvements in the fire-resistant properties. Equilibrium temperature of water-based IC using eggshell (160–260 °C), rice husk ash (180–220 °C), clam shell (136 °C) was reported [43,52,53]. Epoxy resin IC formulated with crop-based carbon source can block the transfer of fire heat to steel and maintain the steel temperature at 130 to 150 °C [28,29]. Calcium carbonate and lignin were the main components found in eggshell/clamshell and ginger/coffee powder, respectively [29,48]. These components had reported an enhancement in the thermal stability and char strength of the IC. It is noteworthy to investigate the potentials of BioAsh (rubberwood ash) that was sourced locally to be renewed as green mineral filler in the development of environmentally friendly water-based IC. Currently, no data can be found in the literature pool concerning the use of rubberwood ash in water-based IC formulation. In this study, performances of fire resistance, thermal, physical, chemical and mechanical properties of green intumescent flame-retarded coating incorporated with BioAsh were evaluated and examined.

2. Materials and Methods

2.1. Raw Materials and Intumescent Coating Samples Preparation

Water-based vinyl acetate copolymer (VAC) was used as the binding agent for BioAsh intumescent coating (IC) in this research. VAC was a milky white emulsion with mean particle size approximate 0.12 µm supplied by Afza Maju Trading, Terrengganu, Malaysia. Three main halogen-free fire-retardant additives: APP, MEL and PER with a mean particle size of 18, <40 and <40 µm, respectively, were supplied by Synertec Enterprise Sdn Bhd, Kuala Lumpur, Malaysia. Titanium dioxide (TiO₂) with a particle size < 10 µm was used as an industrial flame-retardant white pigment in the formulation. TiO₂ was supplied by Chemolab Supplies Sdn Bhd., Selangor, Malaysia. BioAsh was used as the natural substitute of flame-retardant mineral fillers in the IC formulations due to it consisting of a group of high thermal stability elements [37]. Sieve analysis was used to identify the particle size of BioAsh and the most abundant particle size of 300 µm was obtained. BioAsh with weight percentage of 1.0, 3.5, 5.0 and 10.0 wt.%, respectively, were incorporated to the IC samples as shown in Table 1.

Table 1. Formulation of BioAsh intumescent coating samples.

Sample	VAC (wt.%)	Flame-Retardant Additives: APP:PER:MEL (wt.%)	Mineral Fillers (wt.%)	
			Industrial: TiO ₂	Green: BioAsh
BAIC 1-0	50	20:10:10	9.0	1.0
BAIC 3-5	50	20:10:10	6.5	3.5
BAIC 5-0	50	20:10:10	5.0	5.0
BAIC 10-0	50	20:10:10	-	10.0

BioAsh intumescent coating (BAIC) samples were formulated in the laboratory. Respective raw ingredients were mixed using a high-speed disperser at 1500 rpm for 60 min to achieve a homogenous

status. BAIC samples, namely, BAIC 1-0, BAIC 3-5, BAIC 5-0 and BAIC 10-0, were synthesized for investigation.

2.2. Fire Resistance Test

The fire-protective performance of BAIC sample was investigated via 60 min of burning test. This experimental setup test was conducted in a fume hood within a confine zone in the laboratory. The formulated BAIC was applied using a hand brush onto a carbon steel plate with the dimensions of 100 mm (length) \times 100 mm (width) \times 2.0 mm (thick) to cure in an air-dried condition for 7 days. This procedure was continued for 5 to 7 times until an end thickness of 1.5 ± 0.2 mm dry film IC was acquired. The dry film IC was measured using a digital Vernier caliper. An auto ignition blowtorch gun- IDEALGAS Laser-3000 from Idealgas, Casier, Italy installed with EN417 butane gas cartridge from Providus, Volpiano, Italy was used for the burning test. Maximum gas consumption was 150 g/h. The coated steel plate was held in a vertical position using a three-finger clamp and exposed to a 1000 °C high-temperature flame from a blowtorch gun. The valve of the blowtorch gun was adjusted to 60% of its maximum to stabilize the pressure of the gas tank for 60 min. The distance between the BAIC-sample-coated steel plate and fire from the blowtorch was 70 mm. The temperature of the BAIC-coated steel plate was recorded in degree Celsius, measured by a digital thermometer connected to a thermocouple attached at the backside of the carbon steel plate. Fire resistance tests were conducted triplicate for each sample to obtain the mean temperature. The fire resistance test was set up as shown in Figure 1.

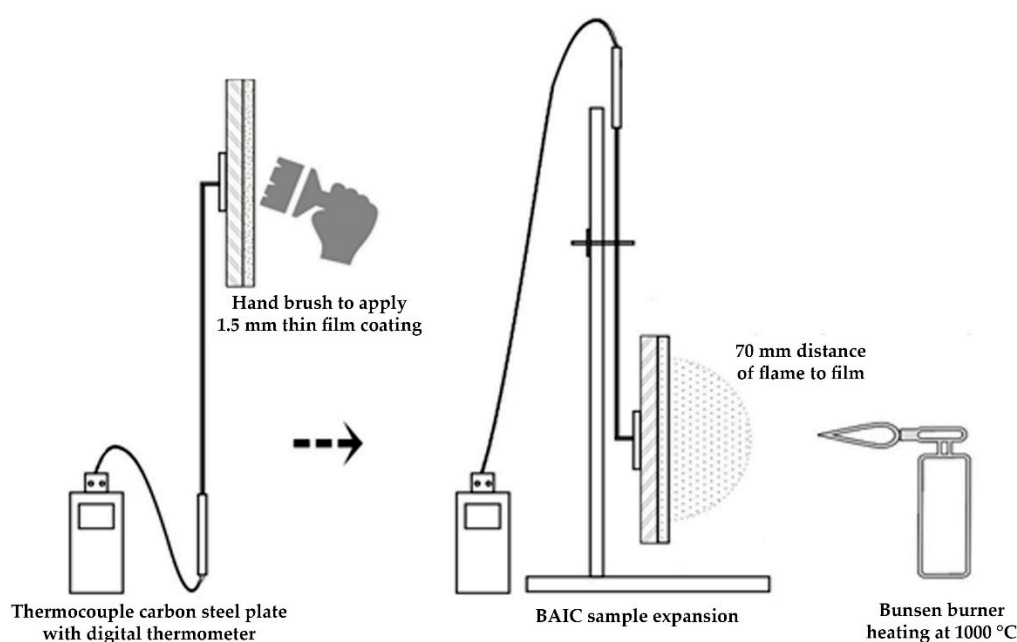


Figure 1. Fire resistance test.

2.3. Carbolite Furnace Test

BAIC sample exposed to a temperature at 600 °C was examined [50]. 1.5 ± 0.2 mm thin film BAIC was hand brushed onto a steel plate size 50 mm (length) \times 50 mm (width) \times 20 mm (thick) and air dried at room temperature for 7 days. The thickness of the dry film was measured using a digital Vernier caliper. Carbolite furnace model RHF15/8 was used to heat the BAIC sample at a rate of 50 °C per min to determine and evaluate the char thickness formation and fire resistance of BAIC samples after heat treating at 600 °C for a duration of 10 min.

2.4. Thermogravimetric Analysis (TGA)

Thermogravimetric analyzer from Perkin Elmer model STA8000 was used in analyzing the thermal degradation of all samples. The dried BAIC sample weighed between 5 and 10 mg was positioned in a crucible and heated at an elevating temperature from 30 to 1000 °C in a nitrogen gas flow condition. The heating rate was 20 °C/min. Thermal degradation of the sample was examined by measuring the residual weight of the sample upon being exposed to constant heating up to 1000 °C. The mass change of the BAIC sample was measured and calculated to analyze its thermal stability.

2.5. Scanning Electron Microscopy (SEM) and Energy-Dispersive X-ray Spectroscopy (EDX)

Surface morphology of BAIC char layer was analyzed through the projection of a focused beam of electrons in the microscope. Char surface topography, cell size and structural strength of the sample at $\times 2.00$ k magnification was studied. A Scanning Electron Microscope of Hitachi EDAX S3400-N from Hitachi, Tokyo, Japan was used. An ultra-thin gold (Au) film with 2–20 nm thickness was sputter coated onto the sample to enhance the thermal conduction and secondary electron emission. A low beam energy of 1000 V was operated to lower the thermal damage on the char layer of the sample. EDX analysis which accommodated by the SEM device was used to investigate the elemental composition on original BioAsh, wet-dried BioAsh and BAIC samples.

2.6. Fourier Transform Infra-Red Spectroscopy (FTIR)

Infrared spectrum absorption and emission of the BAIC sample was analyzed. The presence of functional groups and molecular changes were identified. Nicolet iS10 spectrometer from Thermo Fisher Scientific was used. An infrared spectra wavenumber between 1000 and 4000 cm^{-1} was studied.

2.7. Freeze–Thaw Cycle Test

The stability of the BAIC sample towards changes of various physical weathering conditions was tested. 1.5 ± 0.2 mm thin film sample was hand brushed onto a steel plate of 50 mm (length) \times 50 mm (width) \times 1 mm (thick) and air dried for 24 h. The sample was settled in air temperature at 27 °C for 2 h and quickly frozen in a freezer at -20 °C for 2 h. This was followed by heating the sample in a drying oven at 50 °C for 2 h. A total of 70 cyclic freeze–thaws were conducted. Any color changed, fissure, blister, and coagulum on the BAIC samples were observed and recorded.

2.8. Static Immersion Test

Water resistance of the BAIC thin film sample was evaluated. The sample was immersed in distilled water in an enclosed container at room temperature. For every 1-h interval, the sample was withdrawn and blotted dry with a paper towel, any water on the surface was eliminated. Weight change of the sample was measured using the gravimetric device and calculation was made following Equation (1):

$$E_{sw} = [(W_e - W_o)/W_o] \times 100\% \quad (1)$$

where E_{sw} indicates the water uptake ratio of the sample, W_e indicates the wet weight of the sample at various time, and W_o indicates the initial dry weight of the sample. The water absorption of the BAIC sample was examined every one-hour interval with a total duration of up to 5 h.

2.9. Instron Pull-off Adhesion Test

Interfacial bonding of BAIC sample with the steel plate was investigated via Instron Universal Testing machine model 3400 from Illinois Tool Works, IL, USA. The 1.5 ± 0.2 mm thin film BAIC sample was applied onto the surface of a cylindrical steel rod with 8.03×10^{-4} mm^2 cross-sectional area and cured at room temperature. The steel rod surface coated with BAIC sample was then adhered to the plain surface of another steel rod using epoxy glue and air-dried for 24 h. The tensile pull-off adhesion

test was conducted by applying a perpendicular tensile force to detach the BAIC sample from the steel rod surface with a consistent speed rate at 1 mm/min. Adhesion strength (f_b) of the sample was analyzed in compliance with American Society for Testing and Materials (ASTM) D4541 standard based on Equation (2):

$$f_b = F/A \quad (2)$$

where f_b indicates the adhesion strength (MPa), F indicates the maximum fracture load (N) and $A = \pi(d^2)/4$ indicates the surface area (mm^2) of coated cylindrical steel rod.

3. Results

3.1. Fire Resistance

The fire resistance performances of all BAIC samples were investigated via a Bunsen burner device in a confined fume hood. The end temperatures of all samples after 60 min of burning were tabulated in Table 2. The temperature profiles and standard deviations of all samples are presented in Figure 2.

Table 2. End temperatures of BioAsh intumescent coating (BAIC) samples.

Sample	End Temperature (°C)
Unprotected Steel	796.0
BAIC 1-0	136.3
BAIC 3-5	112.5
BAIC 5-0	159.0
BAIC 10-0	175.7

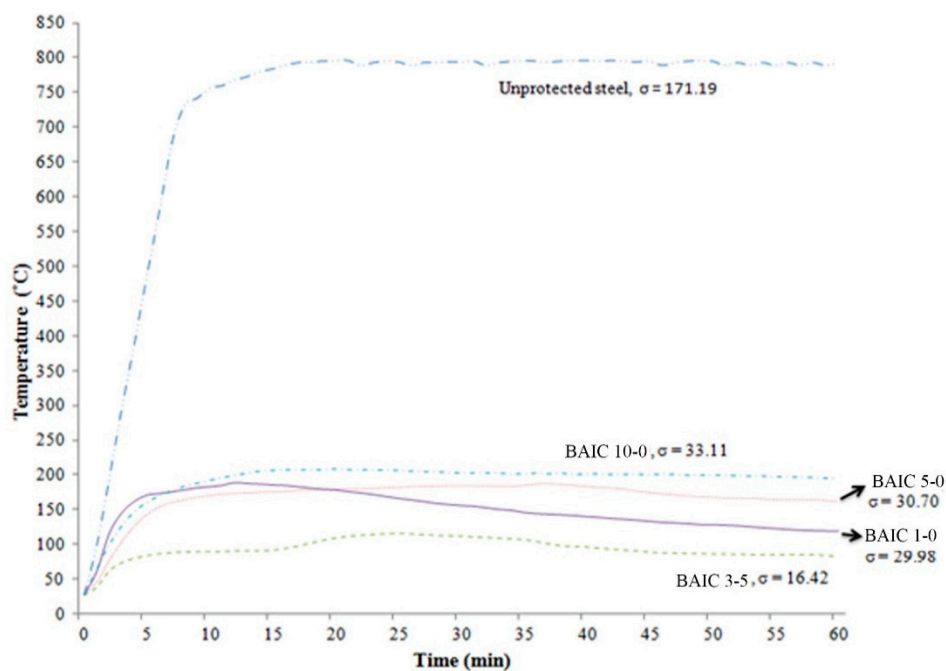


Figure 2. Temperature profiles and standard deviations of unprotected and protected steels with BAIC samples after a one-hour fire resistance test.

BAIC 3-5 had the lowest end temperature and standard deviation (σ) after exposing to a 60-min Bunsen burner test as compared to unprotected steel ($\sigma = 171.19$) and other BAIC coating sample protected steels. BAIC 3-5 exhibited the best fire-resistant outcome at only 112.5 °C and the lowest σ of 16.42 after one hour of fire resistance testing. However, samples BAIC 10-0, BAIC 5-0 and BAIC 1-0

revealed the σ values of 33.11, 30.70 and 29.98, respectively. The elevations of BAIC samples after one hour of fire resistance testing are shown in Figure 3.

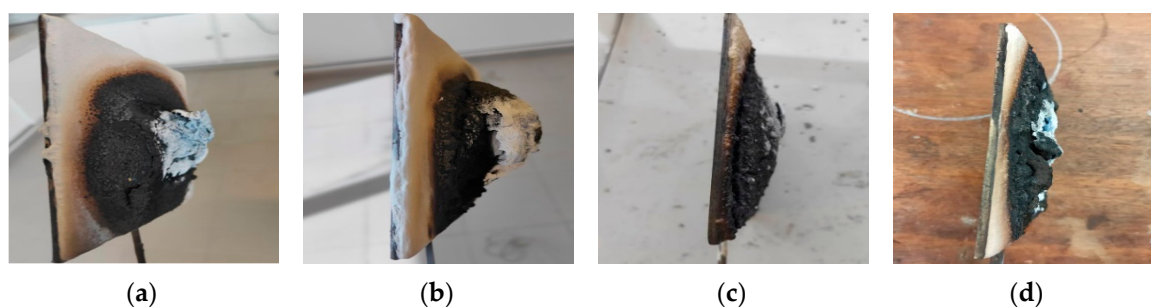


Figure 3. After one-hour fire resistance test: (a) BAIC 1-0, (b) BAIC 3-5, (c) BAIC 5-0, (d) BAIC 10-0.

This result reveals that 3.5 wt.% of BioAsh added into BAIC 3-5 induced an optimum physical and chemical reaction with 6.5 wt.% TiO_2 , and APP-PER-MER/VAC in the formula, resulting in good-quality char with the best fire-resistance outcome. The secondary rise was noticed in BAIC 3-5 after 15 min and returned to equilibrium at 45 min. After 15 min, TiO_2 accumulated at the surface, creating a low emissive material. It changed the boundary condition and thus increased the heat flux received by the material. Fire resistance efficacy was followed by BAIC 1-0 and BAIC 5-0 at 136.3 and 159.0 °C, respectively. BAIC 5-0 started with a lower temperature than BAIC 1-0 in the first 15 min. After 15 min, the temperature of BAIC 5-0 remained equilibrium throughout, whereas BAIC 1-0 was declining in temperature. The decline in burning temperature meaning a more stable char started to take place in BAIC 1-0 only after 15 min. This could be due to a slower char formation process in BAIC 1-0 as compared to others. 9.0 wt.% of TiO_2 added could lower the melt flow rate (MFR) of BAIC 1-0. Low MFR will inhibit gas released from APP-PER-MER/VAC decomposition to expand the carbonaceous char [30]. BAIC 10-0 displayed the worst fire resistance with the highest end temperature at 175.7 °C. This was probably attributable to the elemental composition present in 10.0 wt.% BioAsh that was chemically inert, unable to generate good-quality fire-protective char. This implied single 10.0 wt.% BioAsh in BAIC 10-0 was unideal to activate reaction with APP-PER-MER/VAC formula producing limited poor char to deter heat transmittance. Nonetheless, TiO_2 shall not be used alone as the only mineral filler in IC formula as this led to poor adhesion strength of the coating to the steel, exposed the steel to fire resulted in bad fire resistance [31]. The combination of mineral fillers (hybrids) in IC formulation was required and crucial to ensuring a promising fire-resistance outcome and adhesion strength to the steel [31]. All steel plates coated with BAIC coating samples displayed a better fire resistance efficiency (below 200 °C) than unprotected steel plate that raised to the maximum temperature of 796 °C when exposed to 60 min of fire [13,31]. All BAIC samples did not detach from the steel plate. This indicated an acceptable surface adhesion strength of BAIC samples to the steel surface.

This result reveals that elemental compositions present in 3.5 wt.% BioAsh were able to produce the best synergy effect with 6.5 wt.% TiO_2 in APP-PER-MER/VAC formula forming the best-quality multicellular char to constrain direct heat transfer to the steel plate. It can be concluded that the hybridization of BioAsh (green flame-retardant mineral fillers) and TiO_2 was appropriate to use to formulate the environmentally friendly IC against fire.

3.2. Char Thickness

Carbolite furnace was used to examine all BAIC coating samples at a temperature of 600 °C. The char thickness of each sample is shown in Figure 4.

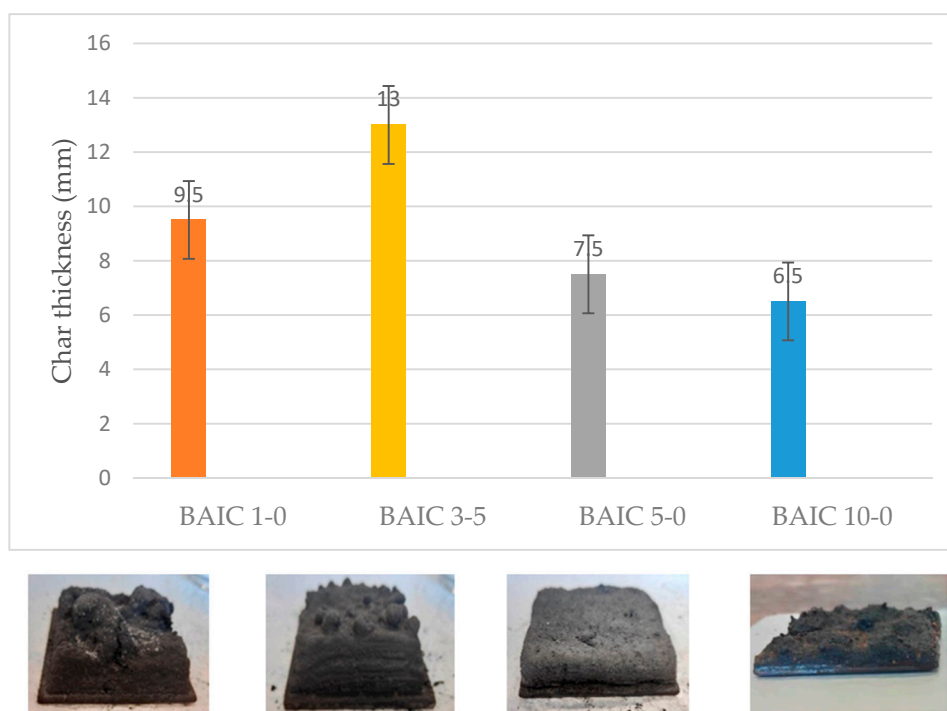


Figure 4. Char thickness (mm) of BAIC samples.

Various ingredients in IC formulation reacted and swelled when exposed to elevated heat. The property and structure of IC changed differently from low to high temperature. 600 °C is determined as the temperature where most of the reactions taken place in IC were finished and an inert char was formed. At a temperature below 600 °C, ingredients in IC were still reacting and complex chemical reactions were in progress. At a temperature above 600 °C, certain ingredients will start achieving their limiting thermal resistance, decompose and turn into ash instead of inert char that is measurable. BAIC 3-5 with 3.5 wt.% BioAsh formed the thickest char layer of 13 mm among the rest. BAIC 1-0, BAIC 5-0 and BAIC 10-0 was 9.5, 7.5, and 6.5 mm thick, respectively. This indicated that BAIC 3-5 formulation under the condition of 3.5 wt.% BioAsh had achieved the optimal reaction with 6.5 wt.% TiO₂ in APP-PER-MER/VAC formula triggered the densest char layer when exposed to heat. This could be largely contributed by the mineral elements and their appropriate composition present in 3.5 wt.% of BioAsh that promote the greatest char thickness. Full replacement of industrial mineral fillers using 10.0 wt.% of BioAsh in BAIC 10-0 led to the thinnest char. Char thickness was not correlated with the increasing amount of BioAsh. The least char expansion in BAIC 1-0 could be attributed to the excessive composition of mineral elements present in 10.0 wt.% BioAsh that suppressed the expansion of desirable char thickness. This research determined an optimum ratio of 3.5 wt.% BioAsh and 6.5 wt.% TiO₂ in the green IC formulation which could ensure the yield of an ideal char thickness to protect the steel from fire.

3.3. Thermogravimetric Analysis

Fire protection performance has correlated with the thermal properties of coating [32]. In this research, thermal degradation of all BAIC samples were examined via TGA. Residual weight vs. temperature of all BAIC samples as plotted in Figure 5. The curves of all samples seem quite similar at the first 100 °C. Obvious thermal decomposition and mass change of all BAIC samples started between 200 and 500 °C indicated by constant drop in curves. The mass loss of BAIC 3-5, BAIC 1-0, BAIC 5-0 and BAIC 10-0 at 500 °C was 60.34%, 61.12%, 63.70% and 66.67%, respectively. Derivative thermogravimetric analysis (DTG) is shown in Figure 6. The peak thermal degradation

of BAIC 3-5, BAIC 1-0, BAIC 5-0 and BAIC 10-0 occurred at a peak temperature of 495, 480, 425 and 400 °C, respectively.

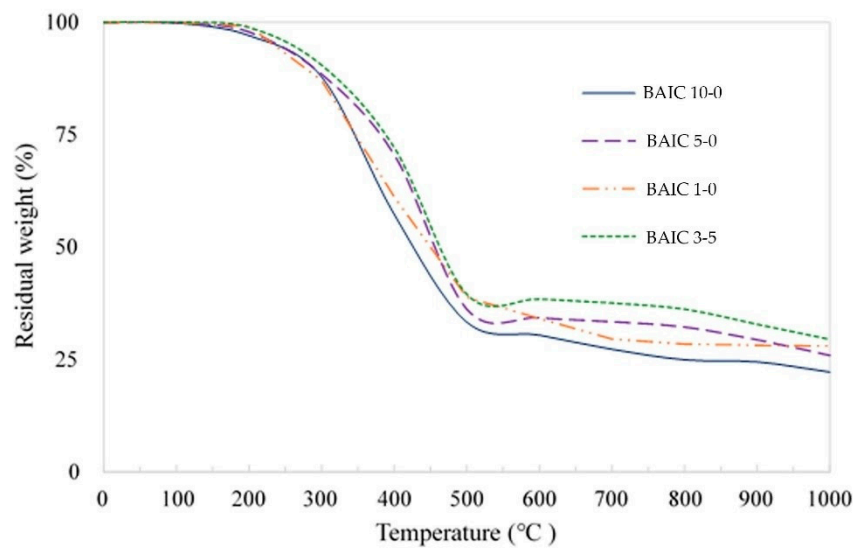


Figure 5. Thermogravimetric analysis (TGA) curves of BAIC samples.

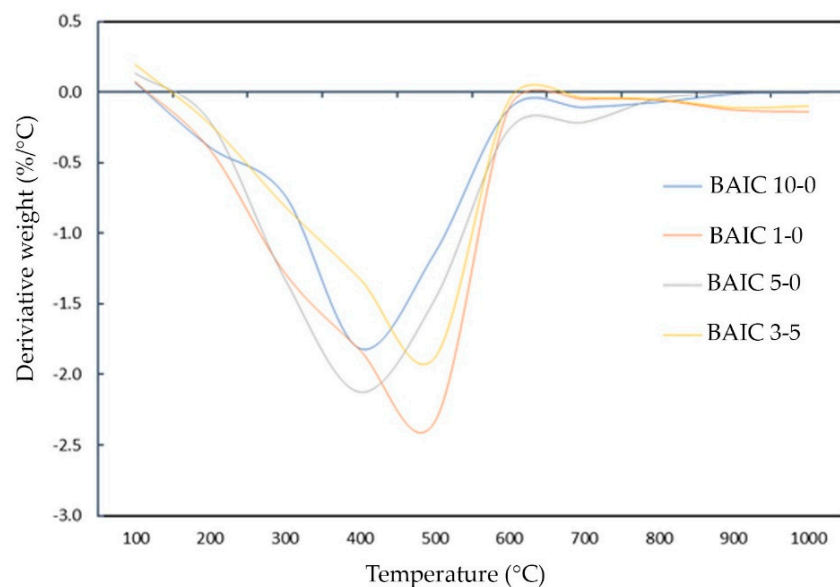


Figure 6. Derivative thermogravimetric analysis (DTG) of BAIC samples.

The potential thermal decompositions of compounds that might take place caused a mass loss of samples, as shown in Table 3 [32–36]. These mineral compounds were predicted from EDX and FTIR analysis of BioAsh of those most likely to undergo thermal decomposition in coating when heat-treated in TGA.

The dominant decomposition was mainly contributed to by the reactive phosphates that contained inorganic $(\text{PO}_4)^{3-}$ ion potentially found in the compound. The phosphates were very reactive; hence, when hydrated and heated, they can react with other elements, creating new compounds transformed into other phosphate forms that were highly soluble, flammable, and volatile. BAIC 3-5 had the highest residual weight of 29.48 wt.%, followed by BAIC 1-0 of 27.99 wt.% and BAIC 5-0 of 25.93 wt.% at 1000 °C. BAIC 10-0 displayed the lowest residual weight of 24.27 wt.%. BAIC 10-0 supplemented with 10.0 wt.% BioAsh degraded the most. BAIC 1-0 had a higher residual weight than BAIC 5-0 at the end of the test. BAIC 1-0 with filler combination of 1.0 wt.% BioAsh and 9.0 wt.% TiO_2

performed better than BAIC 5-0 with 5.0 wt.% BioAsh and 5.0 wt.% TiO₂. Variables in the residual weight of BAIC samples against high heat had been subjected to different BioAsh: TiO₂ ratio given that APP-PER-MEL/VAC was the fixed parameter. The previous study revealed the use of a suitable amount of eggshell (ES) as filler enhanced thermal properties and char thickness by reducing the heat release rate (HRR), time to ignition (TTI) and total heat release (THR) in the IC [37]. The primary compound found in ES was calcium carbonate (CaCO₃). A suitable amount of Al(OH)₃, TiO₂ and ES added to IC formulation assisted in lowering the index value of fire propagation [32].

Table 3. Potential compound present in BAIC samples, decomposition reaction and temperature.

Compound	Decomposition Reaction	Decompose Temperature (°C)
CaCO ₃	CaCO ₃ → CaO + CO ₂	700
Mg(OH) ₂	Mg(OH) ₂ → MgO + H ₂ O	360
Al(OH) ₃	Al(OH) ₃ → Al ₂ O ₃ + H ₂ O	180
2H ₃ PO ₄	2H ₃ PO ₄ → H ₄ P ₂ O ₇ + H ₂ O	200
4AlPO ₄	4AlPO ₄ → 2Al ₂ O ₃ + P ₄ O ₁₀	100
Mg(H ₂ PO ₄) ₂	Mg(H ₂ PO ₄) ₂ → MgH ₂ P ₂ O ₇ + H ₂ O	450
-C ₂ H ₅ -	-C ₂ H ₅ - → -C ₂ H ₄ - + H ⁺	95

This research predicted the proper combination of CaCO₃ and Al(OH)₃ presence in 3.5 wt.% BioAsh and 6.5 wt.% TiO₂ could enhance the thermal stability of BAIC 3-5 as compared to the rest. This research concluded that the synergistic reaction of 3.5 wt.% BioAsh with 6.5 wt.% TiO₂ in the formulation was able to lower the thermal degradation of BAIC 4-7 from more heat in TGA. HRR, TTI, THR of BAIC samples in accordance with BS476 Part 6: Fire propagation test will subject to future investigation.

3.4. Surface Morphology

Char surface morphology of all BAIC samples after Bunsen burner test were investigated under high magnification of ×2.00 k in SEM. Surface micrographs of all samples as shown in Figure 7.

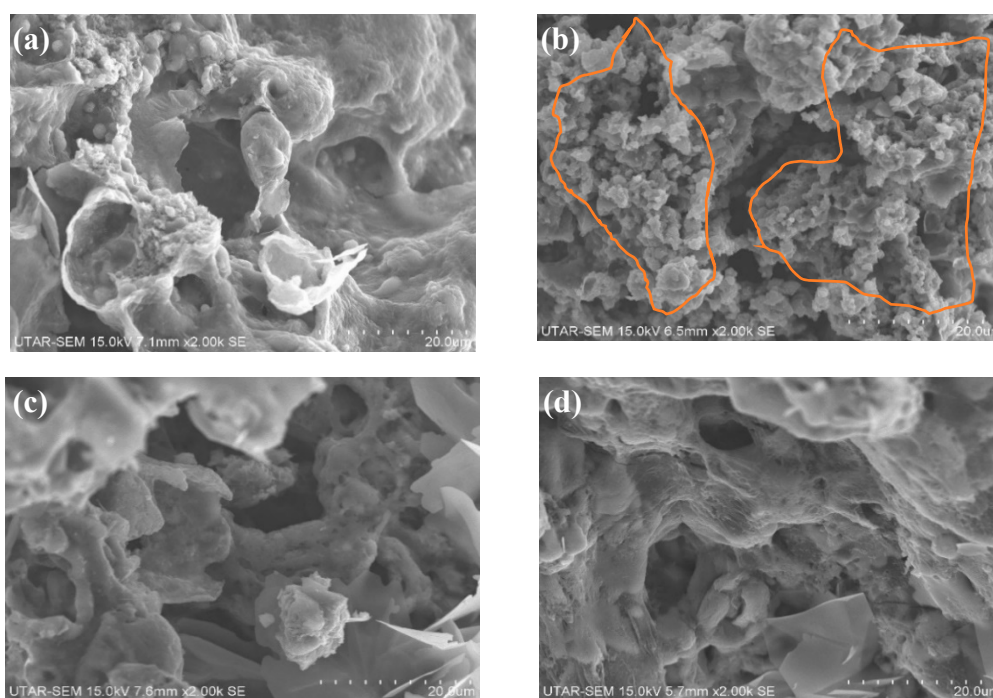


Figure 7. Char morphology: (a) BAIC 1-0, (b) BAIC 3-5, (c) BAIC 5-0 and (d) BAIC 10-0.

Char layer quality of samples was analyzed. BAIC 3-5 showed a more compact and solid char structure among all samples. Char of BAIC 3-5 displayed a multicellular rosette-like crystalline structure that was rigid with minimal micropores [38]. Complex physical and chemical characteristics of wood ash when hydrated will expand and result in a rosette-like structure. This rosette-like form will remain after being air dried [38]. The multicellular rosette-like crystalline char structure indicated that BAIC 3-5 added with 3.5 wt.% BioAsh was able to form a more solid and uniform carbonaceous matrix resulting in a better fire-protective barrier to resist heat transfer. This rosette-like multicellular matrix was occupied with abundant fine void channels (air gaps) that prevented the speedy spread of heat. The rosette-like structure did not present in other samples. In contrast, BAIC 10-0 showed a soft, fluff and filamentous-like char cell that was fragile and with many obvious irregular macro pores. This soft and spongy fibrous-like char structure could be attributed to the high dosage of plant fibers that existed in 10.0 wt.% BioAsh. Non-multicellular and weak char structure happened in BAIC 10-0 accelerated the heat transfer and declined the fire-retardant efficacy. This resulted in the worst fire resistance in BAIC 10-0. Mineral components that present in 10.0 wt.% BioAsh constrained the chemical reactions with TiO_2 in APP-PER-MER/VAC formula. The char structure of BAIC 1-0 displayed fewer macropores and resulted in a better fire-resistant outcome than BAIC 5-0. This research suggests that a suitable mix ratio of BioAsh at 3.5 wt.% and TiO_2 at 6.5 wt.% in the APP-PER-MER/VAC formulation could promote uniform multicellular rosette-like char that was excellent in the fire resistance. An in-depth study into the synergistic and rheological behavior about the formation of unique rosette-like multicellular compacted char using hybridization ratio of BioAsh 3.5 wt.:% TiO_2 6.5 wt.% will subject to future research.

3.5. Elemental Composition Analysis of BioAsh and Coating Samples

Condition of original BioAsh and BioAsh after being wet-dried were analyzed using EDX. Primary mineral contents and changes in wt.% are as tabulated in Table 4. Changes in mineral contents in the original BioAsh and BioAsh after being wet-dried were identified in Figure 8.

Table 4. Primary elemental composition change of original BioAsh and BioAsh after being wet-dried.

Sample	Element (wt.%)										
	Si	Ca	Mg	Al	P	C	Zn	S	Ru	O	Ga
BioAsh (original)	1.26	11.59	3.10	-	5.22	41.13	1.08	1.66	0.94	34.03	-
BioAsh (wet-dried)	1.57	22.87	5.10	0.65	8.44	21.37	-	-	-	38.31	1.68

Silica (Si) and Calcium (Ca) at 1.26 wt.% and 11.59% were found in the original BioAsh. It was noticed that amount of Si was slightly increased to 1.57 wt.% and the amount of Ca was doubled up to 22.87 wt.% in BioAsh after wet and dried. Minerals such as magnesium (Mg), alumina (Al) and phosphorus (P) in BioAsh were also found increased in amount to 5.10, 0.65 and 8.44 wt.% in a wet-dried condition. Carbon (C) was diminished from 41.13 wt.% to 21.37 wt.% in wet-dried BioAsh. Ca was determined as the primary constituent in rubber tree biomass [38]. Compounds such as CaO , CaCO_3 , $\text{Ca}(\text{OH})_2$, Ca_2SiO_4 were present in wood ash [38]. Various crop-based plant biomasses were examined and chemical compounds such as CaO , SiO_2 , MgO , Al_2O_3 , P_2O_5 were found [40]. EDX findings in this research discovered only the chemical elements in BioAsh. This research assumed that major mineral compounds such as CaO , CaCO_3 and minor mineral compounds such as SiO_2 , MgO , P_2O_5 , Al_2O_3 were potentially present in the original BioAsh. Primary elemental composition changes, where most elements noticed in EDX were increased in volume (except carbon) in hydrated BioAsh involved a series of complicated chemical and physical reactions. Compounds dissolved, decomposed, and forming new compounds caused variation in chemical and physical changes. Potential compounds and their series of complex reactions that might happen in the wet-dried BioAsh were tabulated in Table 5.

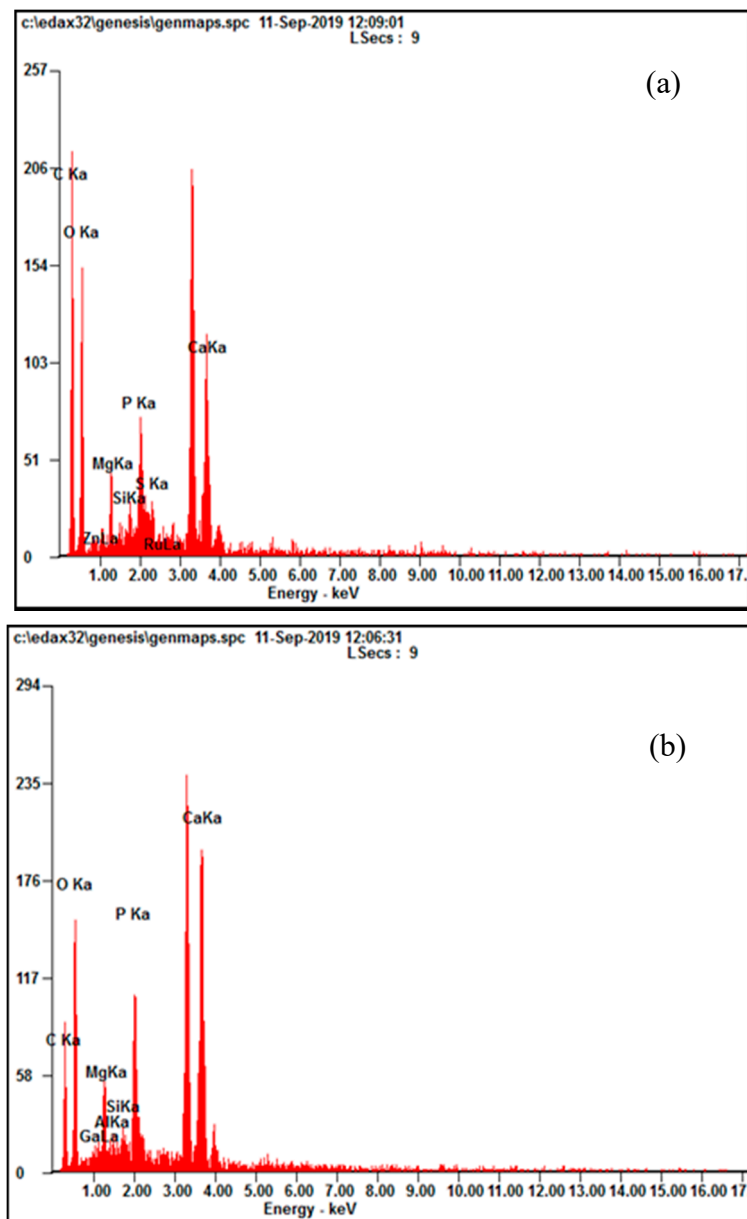


Figure 8. Elemental composition change of (a) original BioAsh and (b) BioAsh after being wet-dried.

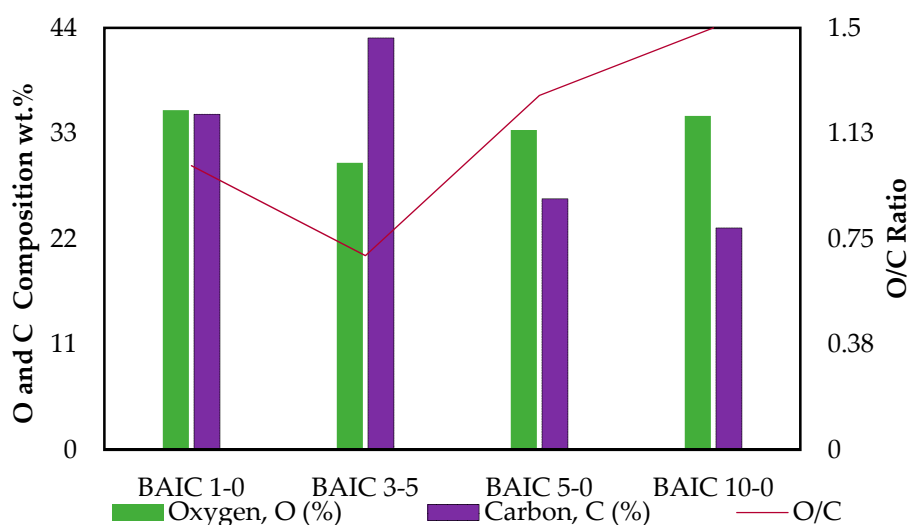
CaO, CaCO₃, and SiO₂ were three main potential mineral compounds that contributed to the formation of Calcium silicate hydrate (C–S–H). C–S–H is a gel-like binding agent accountable to cohere admixture for strength in cementitious materials [51]. Pozzolan shall consist of SiO₂, Al₂O₃ and ferric oxide (Fe₂O₃) as prescribed in ASTM C618. Pozzolanic activities might occur in BioAsh when wetting, converting potential pozzolans SiO₂/CaO/CaCO₃ into a very minor quantity of C–H–S with the cementitious property. Combination of flame-retardant mineral fillers such as Mg(OH)₂ and Al(OH)₃ with an appropriate amount can lower the fire propagation index value, heat release rate and form a more uniform and thicker char layer [37]. Namely, Mg(OH)₂ and Al(OH)₃ that exist in 3.5 wt.% BioAsh might contribute to the best outcomes of BAIC 3-5. Quantitative analysis on the actual amount of Mg(OH)₂ and Al(OH)₃ in 3.5 wt.% BioAsh is necessary in future research.

Table 5. Potential compounds and their reactions occurred during the hydration of BioAsh.

Compound	Chemical Formula	Reaction (Equation)
Carbon	C	$C + O_2 \rightarrow CO_2$
Calcium oxide	CaO	$CaO + H_2O + CO_2 \rightarrow Ca(OH)_2$
	CaO	$3 CaO + SiO_2 \rightarrow Ca_3SiO_5$
Calcium carbonate	CaCO ₃	$CaCO_3 + H_2O \rightarrow Ca^{2+} + CO_2$
Silicon dioxide	SiO ₂	$SiO_2 + H_2O \rightarrow Si(OH)_4$
Calcium hydroxide	Ca(OH) ₂	$Ca(OH)_2 + Si(OH)_4 \rightarrow C-S-H$
	Ca(OH) ₂	$Ca(OH)_2 + CO_2 \rightarrow CaCO_3$
Tricalcium silicate	Ca ₃ SiO ₅ /C ₃ S	$Ca_3SiO_5 + H_2O \rightarrow C-S-H$
Magnesium oxide	MgO	$MgO + H_2O \rightarrow Mg(OH)_2$
Phosphorus pentoxide	P ₂ O ₅	$P_2O_5 + H_2O \rightarrow H_3PO_4$
Aluminum oxide	Al ₂ O ₃	$Al_2O_3 + 3 H_2O \rightarrow Al(OH)_3$

This study reveals that potential elemental compounds and their reactions that took place in 3.5 wt.% BioAsh produced the most positive synergic effect with 6.5 wt.% TiO₂ in APP-PER-MEL/VAC formula in enhancing the fire-resistance properties.

Oxygen and carbon composition of all BAIC coating samples were examined via EDX. The oxygen to carbon ratio is shown in Figure 9.

**Figure 9.** Oxygen and carbon composition, and O/C ratio of BAIC samples.

Oxygen to carbon ratio was crucial in investigating the antioxidation property of the char layer [41]. BAIC 3-5 reinforced with 3.5 wt.% BioAsh had achieved the lowest O/C ratio at only 0.69, which was able to slow down the fire and heat propagation toward the steel underneath it. BAIC 3-5 manifested the best fire-resistant, furnace and TGA outcomes. In contrast, BAIC 10-0 sample with 10.0 wt.% BioAsh displayed the highest O/C ratio at 1.50 demonstrated the weakest performance to resist fire. Char layer of BAIC 10-0 oxidized tremendously caused the loss of electrons damaged the molecules in char cells. SiO₂ and Al₂O₃ predicted present in the BioAsh were known for their antioxidant properties. SiO₂ and Al₂O₃ in BAIC 3-5 might be assisted in the best synergy with TiO₂-APP-PER-MEL/VAC that enhanced the antioxidant quality of the char layer formed. This research suggested, 3.5 wt.% of BioAsh in BAIC 3-5 was appropriate to offer an excellent antioxidant value to enhance the charred quality to better suppress the heat transfer to steel [52].

3.6. FTIR Analysis

FTIR was used to characterize the cross linkage of molecular functional groups in all BAIC samples. The relationship of functional groups with adhesion strength then can be diagnosed [42]. Analysis of elemental functional groups with the peak wavenumber and band position of all BAIC samples is shown in Figure 10.

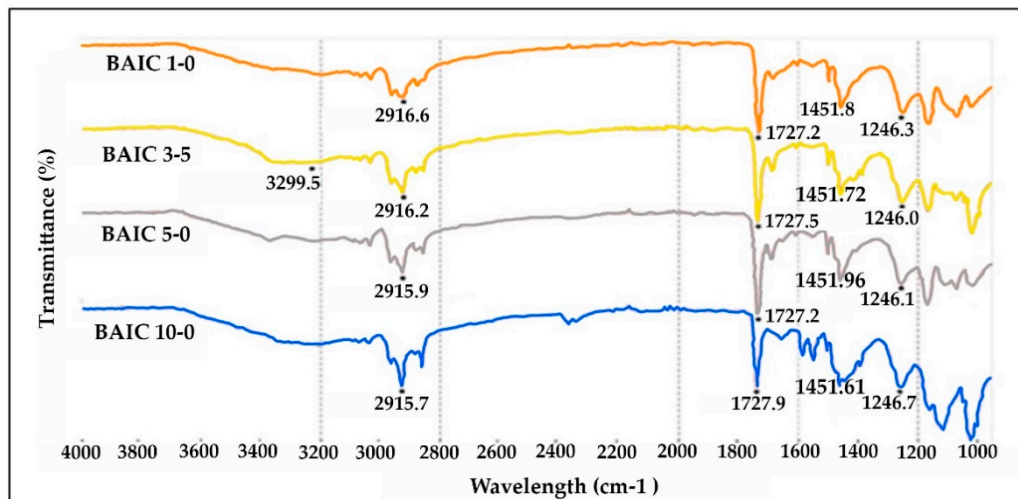


Figure 10. Infrared spectra of BAIC samples.

BAIC samples incorporated with a different weight percentage of BioAsh exhibited variation in peak position. Peak ranging from 2915.7 to 2916.6 cm^{-1} indicated the symmetrical stretching of C–H of alkyl chain in the methyl group [42]. Stretching of C=O (carbonyl group) in lignin and hemicellulose that originated in BioAsh (rubberwood biomass) displayed at peak 1727.2 to 1727.9 cm^{-1} . –C–O (ester bond) and –C=O (ester carbonyl) that were sensitive to form a hydrogen bond can be found in vinyl acetate copolymer. The transmittance of –C–O and –C=O showed peaks ranging from 1246.0 to 1246.7 cm^{-1} and 1727.2 to 1727.9 cm^{-1} , respectively, in all BAIC samples proving the formation of hydrogen bonds [39]. The peak from 1246.0 to 1246.7 cm^{-1} proved the deformation of the carbonyl group (C–H) present in cellulose, hemicellulose, and lignin [29]. Aromatic ring in lignin was identified at the peak from 1600 to 1585 cm^{-1} and 1500 to 1400 cm^{-1} [44]. All BAIC samples showed a peak between 1451.61 and 1451.96 cm^{-1} that manifested the stretching of C=C (aromatic ring) in lignin present in BioAsh. Lignin reported a decomposition temperature of 150–900 °C in the TGA [22,54,55]. This wide range of decomposition temperatures of lignin further predicted its present in the BAIC samples. Polymer compounds associated with aromatic rings such as lignin are reported to be advantageous for thermal stability and char barrier formation [45]. Wide band position from 3100 to 3600 cm^{-1} was exhibited in all samples. This could be attributed to the stretching of the hydroxyl group (O–H) [46] that derived from intense intermolecular and intramolecular of hydrogen bonds. This O–H functional group could contribute to the interfacial hydrogen bonding between BAIC samples and the steel surface [47].

3.7. Freeze–Thaw Cycle

Any cracking, color change, blister, and coagulum on all BAIC coating samples were visually assessed. The appearance of BAIC 1-0, BAIC 3-5, BAIC 5-0, BAIC 10-0 after 70 freeze–thaw cyclic tests is shown in Figure 11.

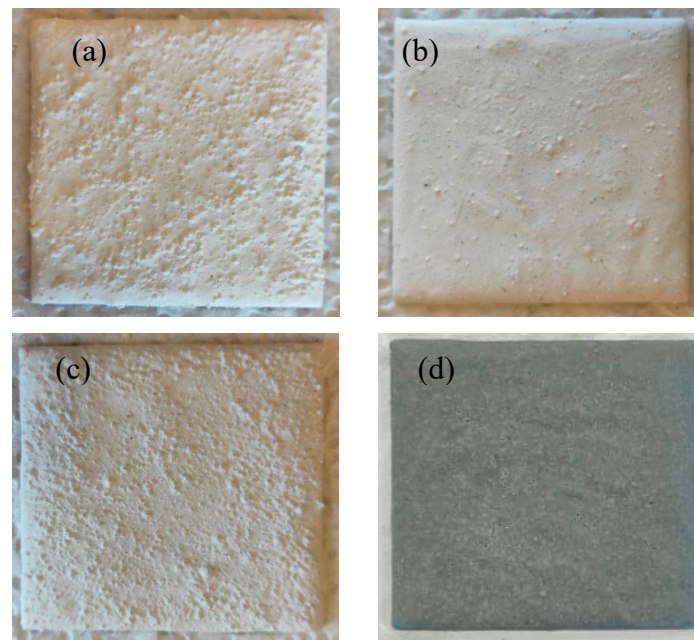


Figure 11. After 70 cyclic tests: (a) BAIC 1-0, (b) BAIC 3-5, (c) BAIC 5-0 and (d) BAIC 10-0.

Obvious coagula were accumulated in BAIC 5-0 and BAIC 1-0. BAIC 3-5 had shown much lesser and finer coagulum in size compared to BAIC 5-0 and BAIC 1-0. These coagula were noticed when the samples were in an air-dried condition before the freeze–thaw cycle test. After the test, coagula in three samples remained unchanged. No coagulum was found in BAIC 10-0. The coagula condition was due to the difference in mix proportion of BioAsh and TiO_2 . Coagula was greatly relevant to the combination of lower BioAsh and higher TiO_2 composition in the formula. All coating samples were attached firmly to the steel plate. No crack, blister and color change were found in all coating samples after the test. This study revealed BioAsh had positive synergy effect with TiO_2 -APP-PER-MEL/VAC on weather resistance of BAIC samples. Other factors could be subjected to very minor C–S–H compound potentially formed from the reactions of SiO_2 , CaO, CaCO_3 that assisted in enhancing the coating's strength against weathering test.

3.8. Static Immersion

Water resistance of all BAIC samples were investigated using static immersion. The weight change of samples during the test was measured every one-hour interval up to 5 h. Water absorption rate of all samples, as shown in Figure 12.

BAIC 3-5 with 3.5 wt.% BioAsh had the lowest water absorption rate at 8.72% with the smallest standard deviation of 2.57 as compared to other samples. The standard deviations of samples BAIC 1-0, BAIC 5-0 and BAIC 10-0 were 5.99, 2.74 and 3.44, respectively. In contrast, BAIC 1-0 exhibited the highest water absorption rate at 19.09% after 5 h. Water permeation in BAIC 1-0 added with 1.0 wt.% BioAsh and 9.0 wt.% TiO_2 was the highest among all. BAIC 10-0 added with 10.0 wt.% of BioAsh had a lower water absorption rate at 10.89% compared to BAIC 1-0. This demonstrated the higher water absorption rate was found to be correlated with the increase in TiO_2 composition. TiO_2 with stronger hydrophilic properties than BioAsh reduced the water resistance by allowing more water particles to penetrate the sample. Inter-surface structure of BAIC samples varied due to different BioAsh: TiO_2 ratio in APP-PER-MEL/VAC formula. BioAsh with a particle size of 300 μm had the largest particles among all ingredients. BAIC 10-0 with the highest portion of 10.0 wt.% BioAsh added forming more pores in the surface structure. Porosity in BAIC 10-0 allowed more water particles (0.275 nm) to penetrate BAIC 10-0, causing decrement in water resistance as compared to BAIC 3-5 and BAIC 5-0. An appropriate ratio of 3.5 wt.% BioAsh and 6.5 wt.% TiO_2 in BAIC 3-5 was able to

slow down the water permeation rate due to the formation of a better particles distribution in the inter-surface matrix. Incorporation of the poorly soluble $\text{Al}(\text{OH})_3$ in IC can help to enhance the water resistance [44]. Hence, it is assumed minor $\text{Al}(\text{OH})_3$ that potentially present in 3.5 wt.% may assist in promoting a better water resistance in BAIC 3-5 without compromising the fire-resistance outcomes. However, hydroxyl groups (O–H), as identified in FTIR can readily form hydrogen bonds to increase the water solubility of the compound. The various number of O–H groups existed in each BAIC coating sample resulted in the different water-resistance performance. BAIC 3-5 was predicted to have the least O–H groups due to its best water resistance among all others.

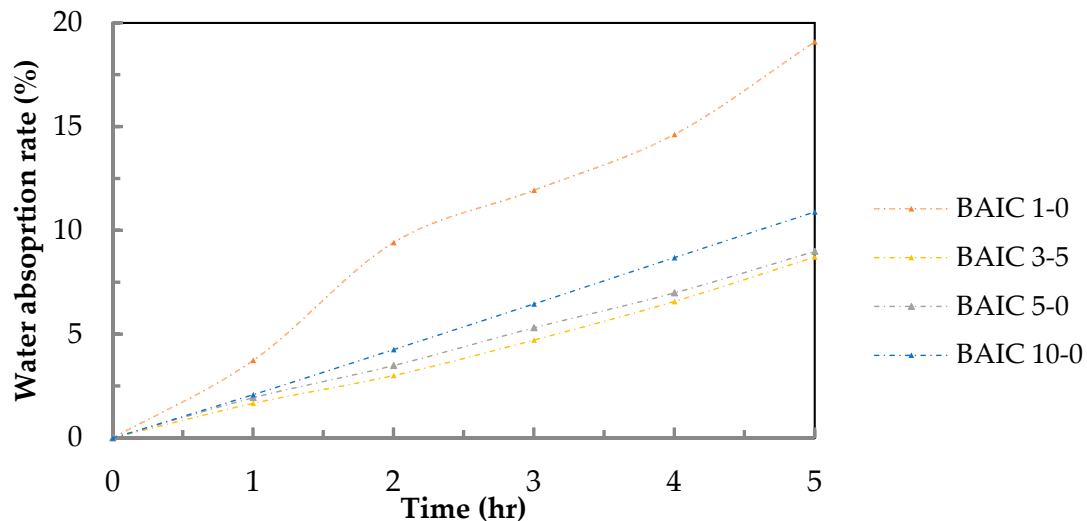


Figure 12. Water absorption rate of BAIC samples.

It can be suggested that the best water resistance of BAIC 3-5 manifested an appropriate amount of 3.5 wt.% BioAsh was more likely to produce a better inter-surface matrix and bonding with TiO_2 -APP-PER-MEL/VAC to minimize the water absorption rate. Water contact angle (wettability) of different BAIC samples, BioAsh, TiO_2 could influence the water-resistance properties and further investigation is required.

3.9. Pull-off Adhesion Strength

Adhesion strength was referred to the physical and chemical bonding of IC samples applied on the steel surface, and the strength required to entirely detach the coating samples from the steel surface. The crack charge value and adhesion strength of all samples are shown in Figure 13.

BAIC 3-5 achieved the highest adhesion strength at 1.73 MPa, followed by BAIC 1-0 at 1.37 MPa and BAIC 5-0 at 1.51 MPa. BAIC 10-0 displayed the lowest adhesion strength value at 1.07 MPa. BAIC 10-0 with 10.0 wt.% BioAsh exhibited the weakest surface bonding to steel. An increment in BioAsh composition was not correlated to an increment in adhesion strength. BAIC 1-0 with 1.0 wt.% BioAsh showed a better adhesion strength to steel surface as compared to BAIC 10-0. This could be attributed to better interfacial bonding between 1.0 wt.% BioAsh, polymer binder and steel surface. The adhesion strength of BAIC 3-5 and BAIC 5-0 was better than BAIC 1-0. A higher amount of TiO_2 at 9.0 wt.% in the formula reduced the adhesion strength of BAIC 1-0 to steel [48]. Single use of TiO_2 as the only mineral filler in the IC formulation was unideal as this will lead to a tremendous loss in adhesion strength of the coating to the steel plate [31]. Hybridization of mineral fillers is required. This study revealed BAIC 3-5 with 3.5 wt.% BioAsh and 6.5 wt.% TiO_2 were able to achieve the best synergic effect of interfacial bonding to the steel surface resulting in the strongest adhesion strength. An appropriate amount of $\text{Mg}(\text{OH})_2$ and CaCO_3 help to improve the adhesion strength of the IC [49]. A stronger bonding between the metal surface and Mg/Ca interface allowed for a better

stress transfer [53]. Magnesium and calcium composition that existed in 3.5 wt.% BioAsh were highly relevant to the best interfacial bonding in BAIC 3-5.

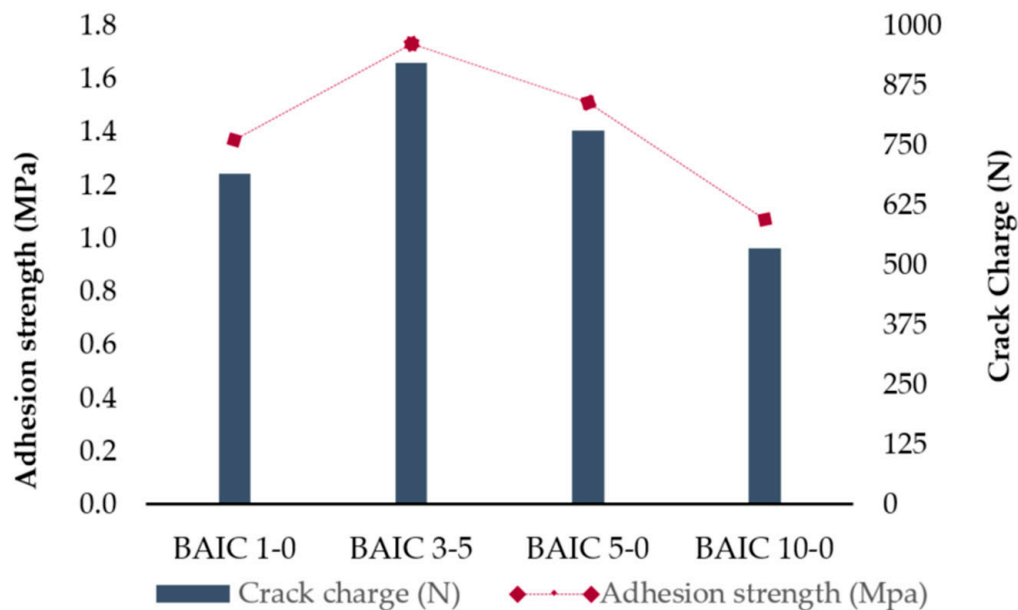


Figure 13. Crack charge and adhesion strength of BAIC c samples.

It can be suggested that an appropriate amount of Mg and Ca elemental composition present in 3.5 wt.% BioAsh were vital to the adhesion strength of the coating to the steel surface. However, $\text{Al}(\text{OH})_3$ in BioAsh will compromise the adhesion strength of the samples. Quantitative analysis of 3.5 wt.% BioAsh was essential in future research. Factors such as variation in the interface region, the structure of atomic bonding, toughness of fracture, purity, and thickness will also have impacts on the adhesion strength.

4. Conclusions

In this research project, all samples BAIC were conducted via the Bunsen burner test, carbolite furnace test, TGA test, FTIR test, SEM/EDX test, Instron pull-off adhesion test, water resistance test and freeze–thaw resistance test to evaluate the performances of fire resistance, mechanical, thermal, chemical and physical properties. Research findings were concluded as follows:

1. BAIC 3-5 sample with 3.5 wt.% BioAsh revealed the best results in fire resistance performance, thermal, physical, and mechanical properties. It had the lowest temperature in fire resistance test at only 112.5 °C, highest residual weight in TGA at 29.48 wt.%, thickest char layer of 13 mm in carbolite furnace test, more uniform and denser multicellular rosette-like char structure present in SEM, lowest water absorption rate and strongest adhesion strength at 1.73 MPa.
2. BAIC 3-5 showed the highest residual weight of 29.48% at 1000 °C in TGA. The synergistic reactions of CaCO_3 and $\text{Al}(\text{OH})_3$ present in 3.5 wt.% BioAsh with 6.5 wt.% TiO_2 -APP-PER-MEL/VAC were able to minimize the thermal degradation from a high temperature.
3. 3.5 wt.% BioAsh in BAIC 3-5 stimulated the carbon composition to 42.96 wt.% and lessened the oxygen composition to 29.93 wt.%, resulting in the lowest O/C ratio against oxidation.
4. All BAIC samples displayed a wide band position at 3100 to 3600 cm^{-1} , indicating the presence of the O–H functional group for interfacial hydrogen bonding to the steel surface. The peak at 1451.61 to 1451.96 cm^{-1} showed in all samples demonstrated the existence of an aromatic ring of lignin present in BioAsh (rubber hardwood ash) accountable for the thermal stability and the formation of good-quality char.

5. The inclusion of BioAsh enabled all BAIC samples to withstand freeze–thaw cycles, which could be attributed to the C–S–H compound formed.
6. The static immersion test showed an appropriate amount of Al(OH)₃ present in BioAsh (3.5 wt.%), hybridized with TiO₂ (6.5 wt.%) in APP-PER-MEL/VAC in BAIC 3-5 enhanced the water resistance. BAIC 3-5 was predicted with the least O-H groups that water solubility was minimized.
7. The significant synergistic effects between 3.5 wt.% BioAsh and 6.5 wt.% TiO₂ in BAIC 3-5 were most stimulated by a series of complex reactions derived from the combination Si, Ca, Mg, Al, P, C and lignin found in the BioAsh. The performance of BAIC 3-5 was the most prominent among all.

Fire protection performance of BAIC 3-5 with lowest equilibrium temperature at 112.5 °C had outstripped the conventional coatings of water-based (220–290 °C) found in the literatures. Moreover, there was 24 °C lowest equilibrium temperature difference between BAIC 3-5 (112.5 °C) and the water-based IC using aquaculture waste (136 °C) reported in the literature. BioAsh contained several elements—Ca, Al, Mg, Si, P, C and lignin (aromatic ring)—at different ratios and significantly enhanced the fire resistance, thermal stability and mechanical strength of BAIC 3-5. These elements that existed in the BioAsh were not commonly reported in the IC formulas using natural-based substances such as clam shell, eggshell and vegetable compounds in the literature. It can be summarized that 3.5 wt.% BioAsh has great potential to be renewed as novel green mineral filler in the IC formulation. The utilization of BioAsh as a natural substitute in the IC could minimize the rely on exotic industrial fillers and contribute to a more sustainable environment.

Author Contributions: Interpretation, J.H.B. and M.C.Y.; methodology, J.H.B.; validation, J.H.B., M.C.Y., M.K.Y. and L.H.S.; formal analysis, J.H.B.; investigation, J.H.B. and M.C.Y.; resources, J.H.B.; data collection, J.H.B.; writing—original draft preparation, J.H.B.; writing—review and editing, M.C.Y.; visualization, M.K.Y. and L.H.S.; supervision, M.C.Y.; project administration, M.C.Y.; funding acquisition, J.H.B. All authors have read and agreed to the published version of the manuscript.

Funding: This project was funded by the Universiti Tunku Abdul Rahman under the Universiti Tunku Abdul Rahman Research Fund (UTARRF).

Acknowledgments: The authors would like to thank Universiti Tunku Abdul Rahman for the Universiti Tunku Abdul Rahman Research Fund (UTARRF), grant number IPSR/RMC/UTARRF/2019-C2/B01 support in this research.

Conflicts of Interest: There is no conflict of interest declared by authors.

References

1. Prabir, B. *Biomass Gasification, Pyrolysis and Torrefaction: Practical Design and Theory*, 3rd ed.; Academic Press: Cambridge, MA, USA, 2018.
2. Sigmann, S.B. Playing with fire: Chemical safety expertise required. *J. Chem. Educ.* **2018**, *95*, 1736–1746. [[CrossRef](#)]
3. Harada, T. Nuclear flash burns: A review and consideration. *Burn. Open* **2018**, *2*, 1–7. [[CrossRef](#)]
4. Altarawneh, M.; Saeed, A.; Al-Harashsheh, M.; Dlugogorski, B.Z. Thermal decomposition of brominated flame retardants (BFRs): Products and mechanisms. *Prog. Energy Combust. Sci.* **2019**, *70*, 212–259. [[CrossRef](#)]
5. Upadhya, S.C. Intumescent coating in the service of fire protection. *Paint India* **2000**, *50*, 45–52. Available online: <https://pascal-francis.inist.fr/vibad/index.php?action=getRecordDetail&idt=831167> (accessed on 8 September 2020).
6. Bourbigot, S.; Le Bras, M.; Duquesne, S.; Rochery, M. Recent advances for intumescent polymers. *Macromol. Mater. Eng.* **2004**, *289*, 499–511. [[CrossRef](#)]
7. Zia-ul-Mustafa, M.; Ahmad, F.; Ullah, S.; Amir, N.; Gillani, Q.F. Thermal and pyrolysis analysis of minerals reinforced intumescent fire retardant coating. *Prog. Org. Coat.* **2017**, *102*, 201–216. [[CrossRef](#)]
8. Amir, N.; Ahmad, F.; Megat-yusoff, P.S.M. Study on the fibre reinforced epoxy-based intumescent coating formulations and their char characteristics. *J. App. Sci.* **2011**, *11*, 1678–1687. [[CrossRef](#)]
9. Duquesne, S.; Magnet, S.; Jama, C.; Delobel, R. Intumescent paints: Fire protection coatings for metallic substrates. *Surf. Coat. Technol.* **2004**, *302*, 180–181. [[CrossRef](#)]

10. Duquesne, S.; Magnet, S.; Jama, C.; Delobel, R. Thermoplastic resins for thin film intumescent coatings—towards a better understanding of their effect on intumescent efficiency. *Polym. Degrad. Stab.* **2005**, *88*, 63–69. [[CrossRef](#)]
11. Yang, H.; Yu, B.; Song, P.; Maluk, C.; Wang, H. Surface-coating engineering for flame retardant flexible polyurethane foams: A critical review. *Compos. Part B Eng.* **2019**, *176*, 107–185. [[CrossRef](#)]
12. Wang, G.; Yang, J. Influences of binder on fire protection and anticorrosion properties of intumescent fire resistive coating for steel structure. *Surf. Coat. Technol.* **2010**, *204*, 1186–1192. [[CrossRef](#)]
13. Yew, M.C.; Ramli Sulong, N.H. Fire-resistive performance of intumescent flame-retardant coatings for steel. *Mater. Des.* **2012**, *34*, 719–724. [[CrossRef](#)]
14. Yew, M.C.; Ramli Sulong, N.H.; Yew, M.K.; Amalina, M.A.; Johan, M.R. Fire propagation performance of intumescent fire protective coatings using eggshells as a novel biofiller. *Sci. World J.* **2014**, *2014*, 805094. [[CrossRef](#)] [[PubMed](#)]
15. Jimenez, M.; Duquesne, S.; Bourbigot, S. Characterization of the performance of an intumescent fire protective coating. *Surf. Coat. Technol.* **2006**, *201*, 979–987. [[CrossRef](#)]
16. Laoutid, F.; Bonnaud, L.; Alexandre, M.; Lopez-Cuesta, J.M.; Dubois, P. New prospects in flame retardant polymer materials: From fundamentals to nanocomposites. *Mater. Sci. Eng. R Rep.* **2009**, *63*, 100–125. [[CrossRef](#)]
17. Hull, T.R.; Witkowski, A.; Hollingbery, L. Fire retardant action of mineral fillers. *Polym. Degrad. Stab.* **2011**, *96*, 1462–1469. [[CrossRef](#)]
18. Natural Rubber Statistic 2018—Malaysia Rubber Board. Available online: [http://www.lgm.gov.my/nrstat/Statistics%20Website%202018%20\(Jan-Dec\).pdf](http://www.lgm.gov.my/nrstat/Statistics%20Website%202018%20(Jan-Dec).pdf) (accessed on 29 June 2020).
19. Rubber Asia: Malaysia for Model Sustainable Rubber Industry. Available online: <https://rubberasia.com/2017/11/28/malaysia-model-sustainable-rubber-industry-dr-zairossani-bin-mohd-director-general-mrb> (accessed on 29 June 2020).
20. Demeyer, A.; Nkana, J.; Verloo, M. Characteristics of wood ash and influence on soil properties and nutrient uptake: An overview. *Bioresour. Technol.* **2001**, *77*, 287–295. [[CrossRef](#)]
21. Tarun, R.N.; Rudolph, N.K.; Rafat, S. *Use of Wood Ash in Cement-Based Materials*; A CBU Report, CBU-2003-19 (REP-513); University of Wisconsin-Milwaukee: Milwaukee, WI, USA, 2003.
22. Waters, C.L.; Janupala, R.R.; Mallinson, R.G.; Lobban, L.L. Staged thermal fractionation for segregation of lignin and cellulose pyrolysis products: An experimental study of residence time and temperature effects. *J. Anal. Appl. Pyro.* **2017**, *126*, 380–389. [[CrossRef](#)]
23. ASTM C 618-05; *Standard Specification For Coal Fly Ash and Raw or Calcined Natural Pozzolans for Use in Concrete*; American Society of Testing and Materials: West Conshohocken, PA, USA, 2005.
24. Ramazani, S.A.A.; Rahimi, A.; Frounchi, M.; Radman, S. Investigation of flame retardancy and physical-mechanical properties of zinc borate and aluminium hydroxide propylene composites. *Mater. Des.* **2008**, *20*, 1051–1056. [[CrossRef](#)]
25. Chuang, Y.J.; Chuang, Y.H.; Lin, C.Y. Fire tests to study heat insulation scenario of galvanized rolling shutters sprayed with intumescent coatings. *Mater. Des.* **2009**, *30*, 2576–2583. [[CrossRef](#)]
26. Suardana, N.P.G.; Ku, M.S.; Lim, J.K. Effects of diammonium phosphate on the flammability and mechanical properties of biocomposites. *Mater. Des.* **2011**, *32*, 1990–1999. [[CrossRef](#)]
27. Han, Z.D.; Fina, A.; Malucelli, G.; Camino, G. Testing fire protective properties of intumescent coating by in-line temperature measurements on a cone calorimeter. *Prog. Org. Coat.* **2010**, *69*, 475–480. [[CrossRef](#)]
28. De Souza, M.M.; De Sá, S.C.; Zmozinski, A.V.; Peres, R.S.; Ferreira, C.A. Biomass as the Carbon Source in Intumescent Coatings for Steel Protection against Fire. *Ind. Eng. Chem. Res.* **2016**, *55*, 11961–11969. [[CrossRef](#)]
29. De Sá, S.C.; De Souza, M.M.; Peres, R.S.; Zmozinski, A.V.; Braga, R.M.; Melo, D.M.D.A.; Ferreira, C.A. Environmentally friendly intumescent coatings formulated with vegetable compounds. *Prog. Org. Coat.* **2017**, *113*, 47–59. [[CrossRef](#)]
30. Li, H.F.; Hu, Z.W.; Zhang, S.; Gu, X.Y.; Wang, H.J.; Jiang, P.; Zhao, Q. Effects of titanium dioxide on the flammability and char formation of water-based coatings containing intumescent flame retardants. *Prog. Org. Coat.* **2015**, *78*, 318–324. [[CrossRef](#)]
31. Yew, M.C.; Sulong, N.R.; Yew, M.K.; Amalina, M.A.; Johan, M.R. Influences of flame-retardant fillers on fire protection and mechanical properties of intumescent coatings. *Prog. Org. Coat.* **2015**, *78*, 59–66. [[CrossRef](#)]

32. Anna, P.; Marosi, G.; Csontos, I.; Bourbigot, S.; Le Bras, M.; Delobel, R. Influence of modified rheology on the efficiency of intumescent flame retardant systems. *Polym. Degrad. Stab.* **2001**, *74*, 423–426. [CrossRef]
33. Karunadasa, K.S.P.; Manoratne, C.H.; Pitawala, H.M.T.G.A.; Rajapakse, R.M.G. Thermal decomposition of calcium carbonate (calcite polymorph) as examined by in-situ high-temperature X-ray powder diffraction. *J. Phys. Chem. Solids.* **2019**, *134*, 21–28. [CrossRef]
34. Conceicao, T.F.d.; Scharnagl, N. Fluoride conversion coatings for magnesium and its alloys for the biological environment. In *Surface Modification of Magnesium and Its Alloys for Biomedical Applications*, 1st ed.; Sankara-Narayanan, T.S.N., Park, I.-S., Lee, M.-H., Eds.; Woodhead Publishing: Cambridge, UK, 2015; pp. 3–21. [CrossRef]
35. Wypych, G. *Fillers—Origin, Chemical Composition, Properties and Morphology: Handbook of Fillers*, 4th ed.; ChemTec Publishing: Toronto, ON, Canada, 2016.
36. Phosphoric Acid. Wiley Online Library. Available online: <https://onlinelibrary.wiley.com/doi/abs/10.1002/0471743984.vse5529> (accessed on 17 June 2020).
37. Beh, J.H.; Yew, M.C.; Yew, M.K.; Saw, L.H. Fire protection performance and thermal behavior of thin film intumescent coatings. *Coatings* **2019**, *9*, 483. [CrossRef]
38. Etiegni, L.; Campbell, A.G. Physical and chemical characteristics of wood ash. *Bioresour. Technol.* **1991**, *37*, 173–178. [CrossRef]
39. Wang, Y.C.; Zhao, J.P. Facile preparation of slag or fly ash geopolymer composite coatings with flame resistance. *Const. Build. Mat.* **2019**, *203*, 655–661. [CrossRef]
40. Hytonen, J.; Nurmi, J.; Kaakkurivaara, N.; Kaakkurivaara, T. Rubber tree (*Hevea brasiliensis*) Biomass, nutrient content, and heating values in southern Thailand. *Forests* **2019**, *10*, 638. [CrossRef]
41. Kraszkievicz, A.; Kachel-Jakubowska, M.; Niedziolka, I. The chemical composition of ash from the plant biomass in terms of indicators to assess slagging and pollution of surface heating equipment. *Fresenius Environ. Bull.* **2017**, *26*, 6383–6389.
42. Aziz, H.; Ahmad, F. Effects from nano-titanium oxide on the thermal resistance of an intumescent fire retardant coating for structural applications. *Prog. Org. Coat.* **2016**, *101*, 431–439. [CrossRef]
43. Yew, M.C.; Yew, M.K.; Saw, L.H.; Ng, T.C.; Rajkumar, D.; Beh, J.H. Influence of nano bio-filler on the fire-resistive and mechanical properties of water-based intumescent coatings. *Prog. Org. Coat.* **2018**, *124*, 33–40. [CrossRef]
44. Cayla, A.; Rault, F.; Giraud, S.; Salaün, F.; Sonnier, R.; Dumazert, L. Influence of Ammonium Polyphosphate/Lignin Ratio on Thermal and Fire Behavior of Biobased Thermoplastic: The Case of Polyamide 11. *Materials* **2019**, *12*, 1146. [CrossRef]
45. Fan, F.Q.; Xia, Z.B.; Li, Q.Y.; Li, Z. Effects of inorganic fillers on the shear viscosity and fire retardant performance of waterborne intumescent coatings. *Prog. Org. Coat.* **2013**, *76*, 844–851. [CrossRef]
46. Hong, S.M.; Soleimani, M.; Liu, Y.Q.; Winnik, M.A. Influence of a hydrogen-bonding co-monomer on polymer diffusion in poly(butyl acrylate-co-methyl methacrylate) latex films. *Polymers* **2010**, *51*, 3006–3013. [CrossRef]
47. Jessica, J.K.Y.; Yew, M.C.; Yew, M.K. Development of advanced intumescent flame-retardant binder for fire rated timber door. *MATEC Web Conf.* **2020**, *306*, 02006. [CrossRef]
48. Yew, M.C.; Sulong, N.H.R.; Yew, M.K.; Amalina, M.A.; Johan, M.R. Eggshells: A novel bio-filler for intumescent flame-retardant coatings. *Prog. Org. Coat.* **2015**, *81*, 116–124. [CrossRef]
49. Li, G.Q.; Zhang, C.; Lou, G.B.; Wang, Y.C.; Wang, L.L. Assess the fire resistance of intumescent coatings by equivalent constant thermal resistance. *Fire Technol.* **2012**, *48*, 529–546. [CrossRef]
50. Wang, Y.C.; Zhao, J.P. Benign design and the evaluation of pyrolysis kinetics of polyester resin based intumescent system comprising of alkali-activated silica fume. *Prog. Org. Coat.* **2018**, *122*, 30–37. [CrossRef]
51. Devendra, K.; Rangaswamy, T. Determination of mechanical properties of Al₂O₃, Mg(OH)₂ and Sic filled E-glass/epoxy composites. *Int. J. Eng. Res. Appl.* **2012**, *2*, 2028–2033.
52. Li, Y.Z.; Feng, Y.W.; Xu, Z.S.; Yan, L.; Xie, X.J.; Wang, Z.Y. Synergistic effect of clam shell bio-filler on the fire-resistance and char formation of intumescent fire-retardant coatings. *Prog. Org. Coat.* **2020**, *9*, 9479–12030. [CrossRef]
53. Nasir, K.M.; Sulong Ramli, N.H.; Johan, M.R.; Afifi, A.M. Synergistic effect of industrial and bio-fillers waterborne intumescent hybrid coatings on flame retardancy, physical and mechanical properties. *Prog. Org. Coat.* **2020**, *149*, 105905. [CrossRef]

54. Yang, H.; Yan, R.; Chen, H.; Lee, D.H.; Zheng, C. Characteristics of hemicellulose, cellulose and lignin pyrolysis. *Fuel* **2007**, *86*, 1781–1788. [[CrossRef](#)]
55. Lv, D.; Xu, M.; Liu, X.; Zhan, Z.; Li, Z.; Yao, H. Effect of cellulose, lignin, alkali and alkaline earth metallic species on biomass pyrolysis and gasification. *Fuel Process Technol.* **2010**, *91*, 903–909. [[CrossRef](#)]

Publisher's Note: MDPI stays neutral with regard to jurisdictional claims in published maps and institutional affiliations.



© 2020 by the authors. Licensee MDPI, Basel, Switzerland. This article is an open access article distributed under the terms and conditions of the Creative Commons Attribution (CC BY) license (<http://creativecommons.org/licenses/by/4.0/>).